iScience

Article

Pharmacological perturbation of splicing elicits SMG1 reduction: Implications for cancer therapy

Graphical abstract

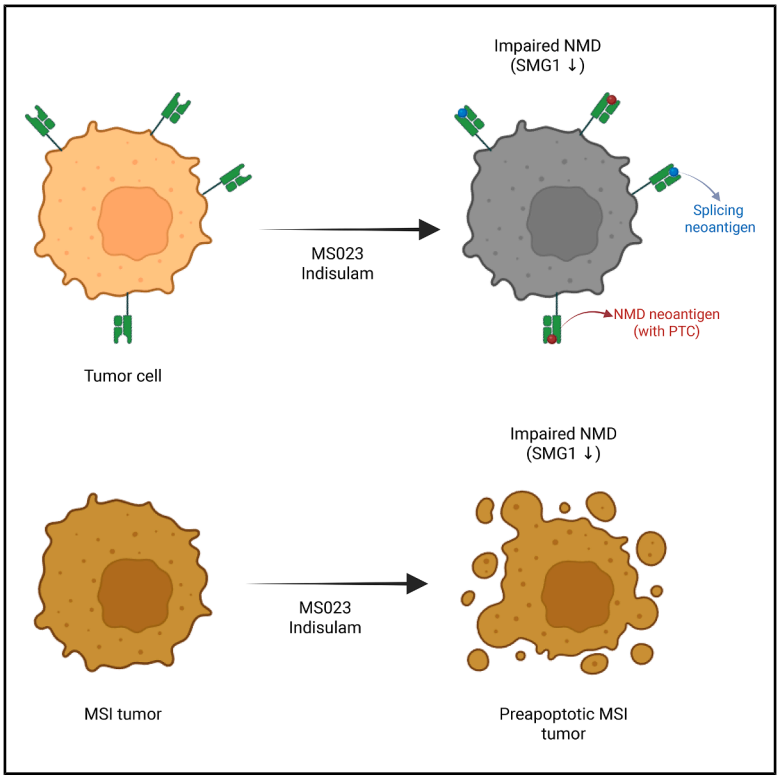

Highlights

- Splicing-modulatory drugs act as NMD inhibitors by downregulating SMG1
- Inhibition of NMD by splicing alteration contributes to the antitumor immune response
- NMD suppression by splicing-modulators exposes a therapeutic vulnerability in MSI tumors
- Key splicing factors show association with SMG1 expression in cancer patients

Authors

Martin Barainka, Angelina Zheleva, Angela Pérez-Cervera, Helena Villanueva, Daniel Meraviglia-Crivelli, Beatriz Moreno, Fernando Pastor

Correspondence

fpasrodri@unav.es

In brief

Immunology; cancer; animal biotechnology

Barainka et al., 2026, iScience *29*, 114597
February 20, 2026
https://doi.org/10.1016/j.isci.2025.114597

CellPress

iScience

CellPress
OPEN ACCESS

Article

Pharmacological perturbation of splicing elicits SMG1 reduction: Implications for cancer therapy

Martin Barainka,[1] Angelina Zheleva,[1] Angela Pérez-Cervera,[1] Helena Villanueva,[1] Daniel Meraviglia-Crivelli,[1] Beatriz Moreno,[1,2] and Fernando Pastor[1,3,4,5,*]

[1]Therapeutic Innovation Program, Center for Applied Medical Research, University of Navarra, Pamplona, Spain
[2]Department of Pathology, Anatomy and Physiology, School of Medicine, University of Navarra, Pamplona, Spain
[3]Instituto de Investigaciones Sanitarias de Navarra (IdiSNA), Pamplona, Spain
[4]Consorcio de Investigación Biomédica en Red de Cáncer (CIBERONC), Madrid, Spain
[5]Lead contact
*Correspondence: fpasrodri@unav.es
https://doi.org/10.1016/j.isci.2025.114597

SUMMARY

Nonsense-mediated mRNA decay (NMD) is an RNA quality control pathway that degrades transcripts containing premature termination codons (PTCs). While the role of NMD in modulating tumor antigenicity and immune evasion is increasingly appreciated, its interaction with splicing remains poorly understood. We uncover a mechanism by which the splicing modulators enhance tumor immunogenicity not only by inducing aberrant splicing events that generate neoantigens but also by suppressing NMD activity through the downregulation of SMG1. This stabilizes PTC-containing transcripts, potentially expanding the pool of neoantigens. Furthermore, we demonstrate that splicing modulation exerts enhanced cytotoxic effects in microsatellite instability (MSI) tumors, which are particularly reliant on NMD for survival. Expression analysis in patient tumors reveals correlations between SMG1 and drug-targeted splicing regulators, supporting a functional link between splicing and NMD. Together, our findings identify splicing modulators as inadvertent NMD inhibitors that simultaneously boost tumor antigenicity and can be used to selectively target NMD-addicted tumors.

INTRODUCTION

Nonsense-mediated mRNA Decay (NMD) is a conserved RNA surveillance mechanism that degrades mRNAs containing premature termination codons (PTCs), which arise from transcription errors, pre-mRNA processing defects, or DNA mutations. NMD activity is initiated by the phosphorylation of UPF1 by SMG1 kinase, a key regulator of the pathway.[1,2] While the role of NMD in cancer has been increasingly studied[3–6] it might be particularly critical in the context of cancer immunotherapy as well as an important vulnerability in some types of tumors that could be considered as NMD-addicted. Certain tumor types may exhibit an NMD-addicted phenotype, meaning they rely on enhanced NMD activity to sustain viability. This dependence has been described in microsatellite instability (MSI) tumors[7] and is likely shared by cancers with high aneuploidy,[8,9] which produce large numbers of defective mRNAs requiring active NMD for cellular homeostasis. Furthermore, it has been observed that some tumors can hijack NMD as a potential mechanism of immune escape[10,11] restricting the tumor antigenicity, and its inhibition induces tumor immunity by unmasking tumor neoantigens.[12]

Tumor neoantigens typically arise from non-synonymous mutations or frameshift mutations, with the latter often generating highly immunogenic peptides due to large sequence alterations.[13] Beyond DNA-level mutations, aberrant RNA processing, especially alternative splicing, represents an important and still underexplored source of tumor antigens, gaining interest more recently. Aberrant splicing events, such as intron retention or exon skipping, usually lead to changes in open reading frames or translation of aberrant intron that, when translated, can be a new source of neoantigens.[14–17] Both splicing modulation and NMD inhibition have independently emerged as promising strategies to enhance tumor immunogenicity[11,12,16,18,19] but never tested in combination.

Pharmacological modulation of splicing using small molecules has gained increasing interest as a translational approach to elicit tumor-specific immune responses and tumor treatment. Few compounds that target splicing have been developed for cancer therapy by different mechanisms,[20,21] and recent studies suggest that some of these agents can actually enhance tumor immunogenicity by inducing novel splicing-derived antigens.[18] For example, MS023 inhibits type-I protein arginine methyltransferases (PRMTs), which modify splicing factors (SRSF2 and SRSF1) through mono- and asymmetric dimethylation, leading to widespread splicing alterations.[21–23] Another compound, indisulam, promotes the degradation of the splicing factor RBM39 through recruitment of the CUL4-DCAF15 E3 ubiquitin ligase complex.[24]

Aberrant splicing often results in the appearance of PTCs due to changes in the open reading frame or due to intron retentions,

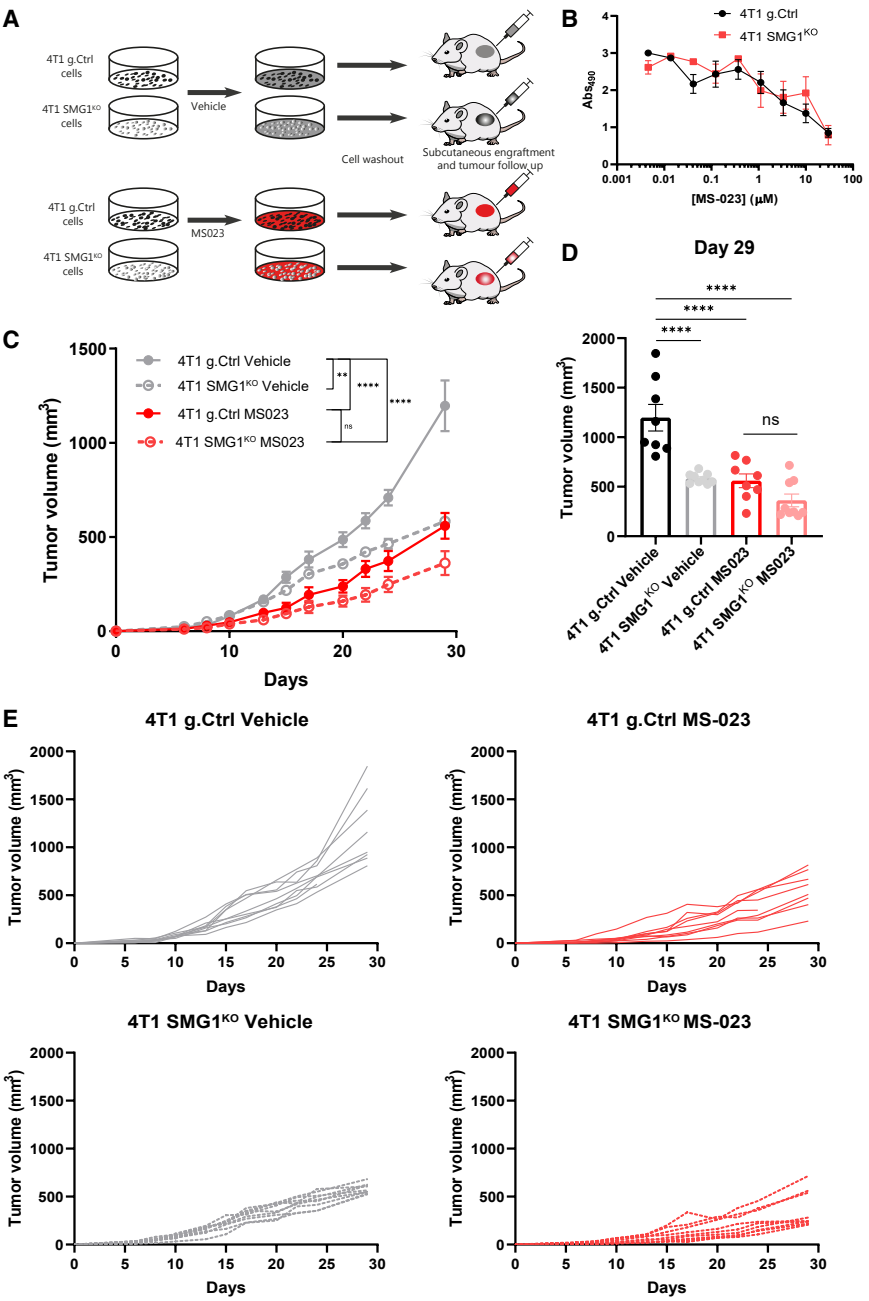

Figure 1. Pharmacological splicing perturbation with MS023 requires NMD activity for full therapeutic efficacy

(A) Schematic representation of the experimental design: 4T1 cells were treated *ex vivo* with MS023 for 96 h prior to implantation into Balb/c mice.

(B) *In vitro* viability assay (MTS) of 4T1 g.Ctrl and SMG1 knockout (SMG1^{KO}) cells treated with increasing concentrations of MS023 for 96 h.

(C) *In vivo* tumor growth of 4T1 g.Ctrl and SMG1^{KO} cells pretreated with MS023 and engrafted into Balb/c mice. Tumor growth was monitored over time (n = 8–10 per group).

(D) Tumor volumes from (C) at the endpoint (day 29).

(E) Individual tumor growth trajectories from (C), showing volume progression for each mouse.

Statistical analysis: two-way ANOVA with Bonferroni's *post hoc* test for tumor growth curves; one-way ANOVA for tumor volume comparisons at endpoint. Data represented as means ± SEM (B–D). ns, not significant; *p < 0.05; **p < 0.01; ***p < 0.001; ****p < 0.0001.

which trigger degradation of the resulting transcripts via the NMD pathway.[1,2] Building on this evidence, we initially hypothesized that although pharmacological splicing modulators can promote neoantigen expression,[18] their full immunogenic potential may be limited by NMD-mediated degradation of PTC-containing transcripts. Intriguingly, in this study, we found that two of these drugs (MS023 and indisulam), in addition to altering splicing, downregulate SMG1 protein levels, thus impairing NMD. This unexpected observation prompted us to reformulate our initial hypothesis. Consequently, no additional therapeutic combination is required, as the pharmacological perturbation of splicing itself by MS023 or indisulam exerts a dual effect: inhibition of NMD and induction of splicing alterations. This positions not only splicing-modulatory drugs, such as MS023 or indisulam, as valuable tools to inhibit splicing but also NMD for cancer immunotherapy and for tumors addicted to NMD.

RESULTS

Pharmacological perturbation of splicing reveals NMD dependencies that reduce tumor growth in an immune-dependent manner

To investigate the contribution of NMD inhibition to the antitumor effect of the splicing modulator MS023, we performed an *in vivo* study using 4T1 murine breast cancer cells with reduced NMD activity. Specifically, we used 4T1 control cells and 4T1 cells with knockout of SMG1 (4T1 SMG1^{KO}), a key kinase required for NMD activation.[11] These cells were pretreated with MS023 (5 μM) for 96 h prior to subcutaneous implantation in Balb/c mice (Figure 1A) as previously done.[18]

To determine cytostatic or cytotoxic effect of the treatment on tumor growth, we performed an MTS viability assay. At 5 μM, the dose used for the *in vivo* experiments, MS023 showed minimal impact on cell viability (Figure 1B). Notably, sensitivity to MS023 was comparable in both SMG1^{KO} and control cells. However, *in vivo*, we observed significant tumor growth delay in mice injected with MS023-treated cells or with SMG1^{KO} cells, compared to untreated controls (p = 0.005 and p < 0.001, respectively). The combination of SMG1 knockout and MS023 treatment showed a further trend toward tumor growth delay,

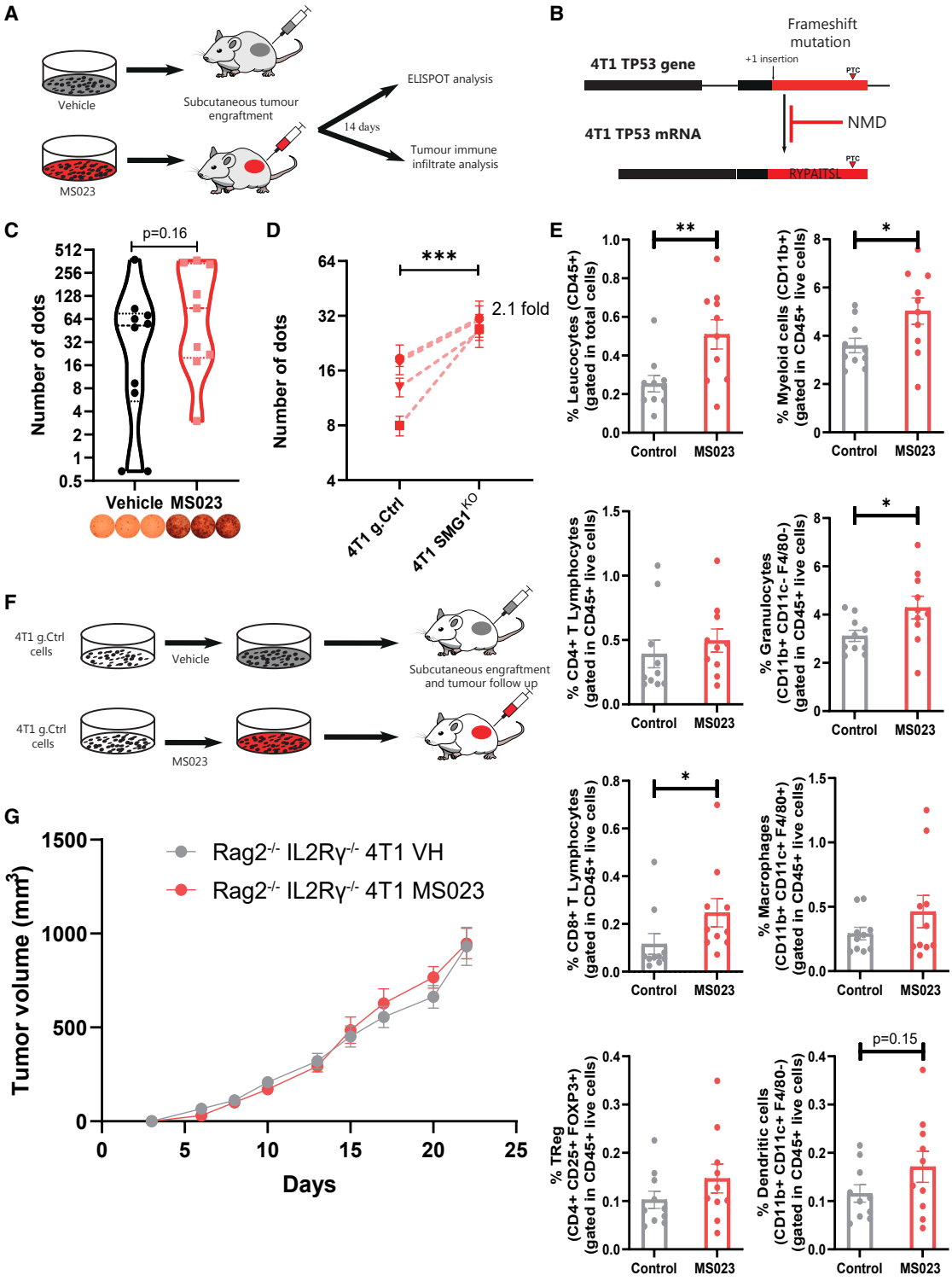

Figure 2. Pharmacological splicing perturbation reduces tumor growth in an immune-dependent manner

(A) Schematic representation of the experimental workflow: 4T1 tumor cells were pre-treated *ex vivo* with the splicing modulator MS023 and subsequently engrafted into Balb/c mice.

(B) Conceptual illustration of peptide generation following NMD inhibition induced by MS023 treatment in 4T1 cells. The figure depicts a frameshift-derived peptide resulting from a +1 insertion mutation in the TP53 gene of 4T1 tumors, which alters the open reading frame and introduces a premature termination codon (PTC) downstream of the insertion.[11]

(legend continued on next page)

although this did not reach statistical significance, suggesting limited additive effects (Figures 1C–1E).

To further explore the effect of splicing modulation, we tested another drug, indisulam, in the highly metastatic B16/F10 melanoma model (Figure S1A). MTS assays performed on B16 SMG1^{KO} and B16 g.Ctrl cells showed comparable cytostatic effects, with 1 μM concentrations being well tolerated in both cases (Figure S1B). In this *in vivo* setting, indisulam alone had modest effects on tumor growth, lower than to SMG1 knockout, and their combination did not enhance the outcome of SMG1 knockout (Figures S1C–S1E). However, when assessing the number of mice that remain alive at day 19 post inoculation, indisulam appeared to improve survival similarly to SMG1^{KO}, with some enhanced protection when combined (Figure S1E).

Since NMD inhibition can promote tumor immunity by stabilizing transcripts bearing PTCs that encode neoantigens,[11,12,19,25] we assessed whether MS023 induces immune responses against such antigens. Balb/c mice implanted with MS023-treated 4T1 cells were sacrificed after 14 days, and the tumor-draining lymph nodes (TDLNs) were analyzed. IFN-γ ELISPOT assays were performed using lymphocytes stimulated with the NMD-dependent neoantigen RYPAITSL,[11] derived from a TP53 frameshift mutation (Figures 2A and 2B). ELISPOT results showed a significantly stronger response in mice implanted with MS023-treated tumors (Figure 2C), suggesting immune recognition of stabilized NMD-dependent neoantigens. Some basal reactivity was also observed in controls, consistent with previous reports of incomplete NMD efficiency.[10,11,26]

To confirm global neoantigen presentation changes, we performed an additional ELISPOT assay using lymphocytes from MS023-treated mice co-cultured with either 4T1 g.Ctrl or 4T1 SMG1^{KO} as feeder cells for antigen presentation. This approach allows the detection of a broader repertoire of NMD-regulated neoantigens. Stronger responses were observed with 4T1 SMG1^{KO} cells (Figure 2D), reinforcing the idea that MS023 enhances immunogenicity through NMD suppression.

Flow cytometric analysis of the tumor immune microenvironment revealed a significant increase in CD45$^+$ leukocyte infiltration in MS023-treated tumors ($p = 0.009$), particularly in CD8$^+$ T cells ($p = 0.04$) and granulocytes ($p = 0.04$), with a trend toward increased myeloid infiltration overall ($p = 0.03$) (Figures 2E and S2).

Finally, to confirm that the antitumor effects of MS023 were immune-mediated, we repeated the *in vivo* experiments in Rag2$^{-/-}$ IL2Rγ$^{-/-}$ immunodeficient mice. No differences in tumor growth were observed between MS023-treated and control groups (Figures 2F–2G, S3A, and S3B), confirming that the therapeutic effects of MS023 are largely dependent on an intact immune system.

Pharmacological alteration of splicing reduces SMG1 protein levels and compromises NMD activity

Based on our *in vivo* findings, we consider that splicing-modulatory drugs may affect NMD. Given that SMG1 is a key kinase that initiates the NMD cascade, and the largest protein involved in this pathway (encoded by a gene of ∼120 kb with 63 exons), we reasoned that it might be particularly vulnerable to splicing alterations due to its complex gene structure.

We first analyzed SMG1 protein levels using western blot in both murine (4T1 and Panc02) and human (ARST) tumor cell lines treated with the splicing modulators, MS023 or indisulam. In all tested cell lines, SMG1 protein levels were reduced upon treatment with these compounds, with a more pronounced decrease observed with MS023 compared to indisulam (Figures 3A–3D).

To assess NMD activity, we employed two complementary approaches: (1) quantification of ATF3 mRNA levels as an endogenous NMD readout[28] (Figure 3E) and (2) a β-globin-based luciferase construct carrying a PTC as a synthetic NMD reporter (Figure 3F). As expected, ATF3 expression was significantly increased after treatment with MS023 or indisulam, consistent with NMD inhibition (Figure 3E).

For the luciferase reporter assay, we generated Panc02 tumor cells stably expressing either a PTC-containing β-globin-luciferase construct or a wild-type β-globin control. Since the PTC variant is subject to NMD, luciferase expression serves as an inverse readout of NMD efficiency (Figure 3F). We observed a significant increase in normalized luciferase signal following treatment with MS023 ($p = 0.001$) and indisulam ($p = 0.0065$), indicating reduced NMD activity (Figure 3G). As a control, the luciferase reporter cells were treated with SMG1i, an inhibitor of SMG1.[19,25,29] Luciferase induction was observed, similar to the results obtained with MS023 or indisulam (Figures S4A and S4B).

To evaluate whether SMG1 splicing is affected at the transcriptome-wide level, we analyzed public RNA-seq data from Lu et al.,[18] in which the human melanoma cell lines (A375, MEL501, and SK-MEL-239) were treated with MS023 or indisulam. Multiple SMG1 splicing alterations were observed across cell lines and treatments. However, the most consistently altered event was the retention of the intron following exon 29 (Figure 3H).

To validate this intron-retention event, we performed RT-qPCR using primers specific for the retained intron in the human melanoma cell line ARST treated with either MS023 or indisulam. A significant increase in intron 29 retention was confirmed following treatment (Vehicle vs. MS023, $p < 0.0001$; DMSO vs. indisulam, $p = 0.004$) (Figures 3I and 3J).

Together, these results confirm that pharmacological modulation of splicing impacts SMG1 transcript processing, leading to

(C) IFN-γ ELISPOT assay was performed using tumor-draining lymph node (TDLN) cells from mice engrafted with MS023-treated 4T1 cells (day 14) and stimulated with the NMD-regulated TP53 peptide ($n = 9$–10 per group).
(D) IFN-γ ELISPOT assay using TDLN cells from mice bearing 4T1 control or SMG1^{KO} tumors ($n = 4$ per group).
(E) Flow cytometry analysis of immune infiltrates in tumors derived from 4T1 cells pre-treated with MS023 for 96 h and harvested on day 14. Each cell population is shown relative to total leukocytes CD45$^+$ and normalized to the processed tumor mass ($n = 9$–10 per group).
(F) Schematic representation of MS023 treatment and engraftment in immunodeficient mice.
(G) Tumor growth curves of 4T1 cells (pre-treated with MS023 for 96 h) implanted into Rag2$^{-/-}$ IL2Rγ$^{-/-}$ mice ($n = 10$ per group).
Statistical analysis: two-way ANOVA with Bonferroni's *post hoc* test (tumor growth); unpaired two-tailed Student's *t* test (ELISPOT and immune infiltrates). Data represented as means ± SEM. ns, not significant; *$p < 0.05$; **$p < 0.01$; ***$p < 0.001$; ****$p < 0.0001$.

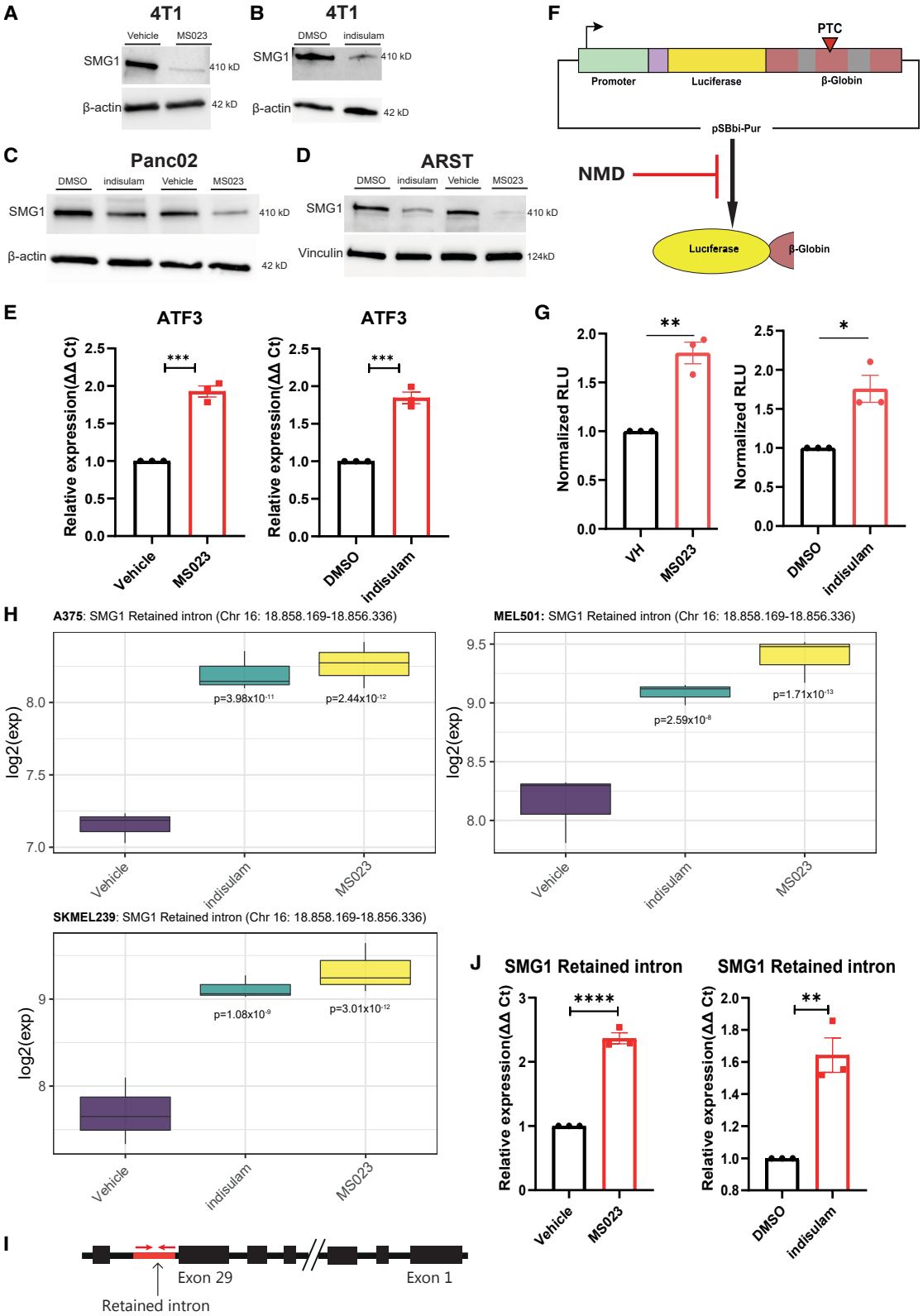

(legend on next page)

reduced SMG1 protein expression and consequent inhibition of NMD activity. This provides a mechanistic link between splicing perturbation and enhanced immunogenicity via impaired NMD.

Pharmacological inhibition of splicing by MS023 or indisulam affects cell viability depending on MSI status

NMD has been proposed not only as a target to enhance antitumor immunity but also as a therapeutic vulnerability in tumors exhibiting MSI.[3,7] Given our previous observation that SMG1 is downregulated in response to splicing-modulatory drugs, we investigated whether this downregulation could affect the viability of MSI versus microsatellite stable (MSS) cancer cells.

To this end, we performed an MTS viability assay in two colorectal cancer cell lines: HCT116 (MSI) and SW480 (MSS), both of which have been previously shown to exhibit differential sensitivity to NMD inhibition.[7] Cells were treated with MS023 or indisulam, and IC50 values were determined (Figures 4A and 4B). The MSI cell line HCT116 showed a significantly lower IC50 than the MSS line SW480, indicating higher sensitivity to splicing modulation.

To determine whether the observed reduction in cell viability was associated with apoptosis, we analyzed apoptosis induction by flow cytometry using Annexin V and Zombie Green staining at 72 h post-treatment (Figure S5). The results confirmed that HCT116 (MSI) cells undergo early apoptosis upon treatment with MS023 or indisulam, in agreement with the MTS assay results (Figures 4C–4F). Furthermore, treatment of HCT116 (MSI) cells with SMG1i resulted in an increase in early apoptotic and dead cells compared to SW480 (MSS) cells (Figure S6), further confirming previous work that NMD inhibition sensitizes MSI cells to splicing modulation.[7]

SMG1 expression is associated with the expression of key splicing factors in cancer patients

Given that SMG1 expression is reduced by splicing-modulatory drugs (MS023 and indisulam), we hypothesized that splicing regulation may be intrinsically linked to NMD activity. Many tumors exhibit altered splicing and heterogeneous expression of key splicing regulators, which could impact SMG1 expression levels.

To explore this possibility, we analyzed single-cell RNA sequencing (scRNAseq) data from tumor cells of a cohort of 31 breast cancer patients,[30] focusing on the expression of SMG1 and different splicing factors. scRNAseq data from Bassez et al.[30] were reanalyzed using the SCTransform normalization method,[31] which corrects for variability in read depth and total mRNA content (Figure 5A). After normalization, SMG1 expression showed positive correlations with key splicing regulators including RBM39, SRSF1, and SRSF2 (Figure 5B). Consistent with this, Gene Set Enrichment Analysis (GSEA) on the ranked correlation list identified "RNA splicing" and "mRNA processing" as top enriched biological processes from Gene Ontology (GO) (Figure 5C), confirming a robust link between SMG1 and druggable splicing machinery in tumor cells. Bulk RNA-seq analysis from The Cancer Genome Atlas (TCGA) datasets further supported these findings (Figure 5D). A similar correlation was seen in a melanoma dataset analysis (Figure S7).[32]

DISCUSSION

Pharmacological modulation of splicing using small molecules has emerged as a promising strategy to induce cryptic neoantigens that enhance antitumor immunity.[16,18] Since many of these neoantigens are generated through the inclusion of PTCs, our initial hypothesis was that splicing modulation could synergize with NMD inhibition, leading to stabilization of aberrant transcripts and increased neoantigen load. Unexpectedly, our results revealed that splicing perturbation alone is sufficient to reduce NMD activity by downregulating SMG1 protein levels, thereby enhancing tumor immunogenicity.

This finding uncovers a new mechanism by which splicing-modulatory drugs such as MS023 and indisulam exert immunomodulatory effects. Specifically, SMG1, a large gene spanning ~120 kb and composed of 63 exons, is highly sensitive to splicing perturbation. We consistently observed the retention of intron 29 in treated tumor cells across multiple models. However, additional intron retention or mis-splicing events throughout the SMG1 transcript are also likely to contribute collectively to the observed reduction in SMG1 protein levels. These splicing-induced defects compromise NMD, as supported by both endogenous and reporter-based NMD assays.

The consequences of pharmacological NMD suppression extend beyond the stabilization of aberrant splicing isoforms. By inhibiting NMD, splicing drugs broaden the tumor immunopeptidome through the accumulation of both cryptic neoantigens and canonical neoantigens derived from frameshift

Figure 3. Pharmacological modulation of splicing reduces SMG1 expression and NMD activity

(A–D) SMG1 protein levels measured by western blot in (A–D) 4T1, (C) Panc02, and (D) ARST cells after 96 h of treatment with MS023 or indisulam.

(E) ATF3 mRNA levels assessed in RT-qPCR in ARST cells treated for 96 h with MS023 or indisulam (n = 3 per group).

(F) Schematic representation of the NMD reporter system: two versions of a plasmid encoding β-globin fused to luciferase were used, one containing a PTC and one without for normalization. The construct bearing the PTC is targeted by the NMD pathway, resulting in decreased luciferase activity, which inversely correlates with NMD activity. Luciferase signal (RLU) in Panc02 cells transfected with the PTC-containing reporter was normalized to signal from cells transfected with the control reporter lacking a PTC (wild-type).

(G) Panc02 cells were stably transduced with either the PTC-containing NMD luciferase reporter or the wild-type (no-PTC) luciferase reporter and treated with MS023 or indisulam for 48 h. The normalized luciferase signal is shown for each treatment condition (n = 3 per group).

(H) RNAseq data[18] from three human melanoma cell lines (A375, MEL501, and SKMEL239) treated with MS023 or indisulam showed accumulation of a SMG1 mRNA variant retaining intron 29, in y axis represent log2-transformed estimated counts, log2(exp), which have been normalized by Sleuth.[27]

(I) Schematic representation of primer design used to detect SMG1 intron 29 retention by RT-qPCR.

(J) RT-qPCR analysis of the intron 29-retaining SMG1 variant in ARST cells after 96 h of treatment with MS023 or indisulam (n = 3 per group).

Statistical analysis: unpaired two-tailed Student's t test was used for comparisons in (E), (G), and (J). Data represented as means ± SEM. ns, not significant; $^{*}p < 0.05$, $^{**}p < 0.01$, $^{***}p < 0.001$, $^{****}p < 0.0001$.

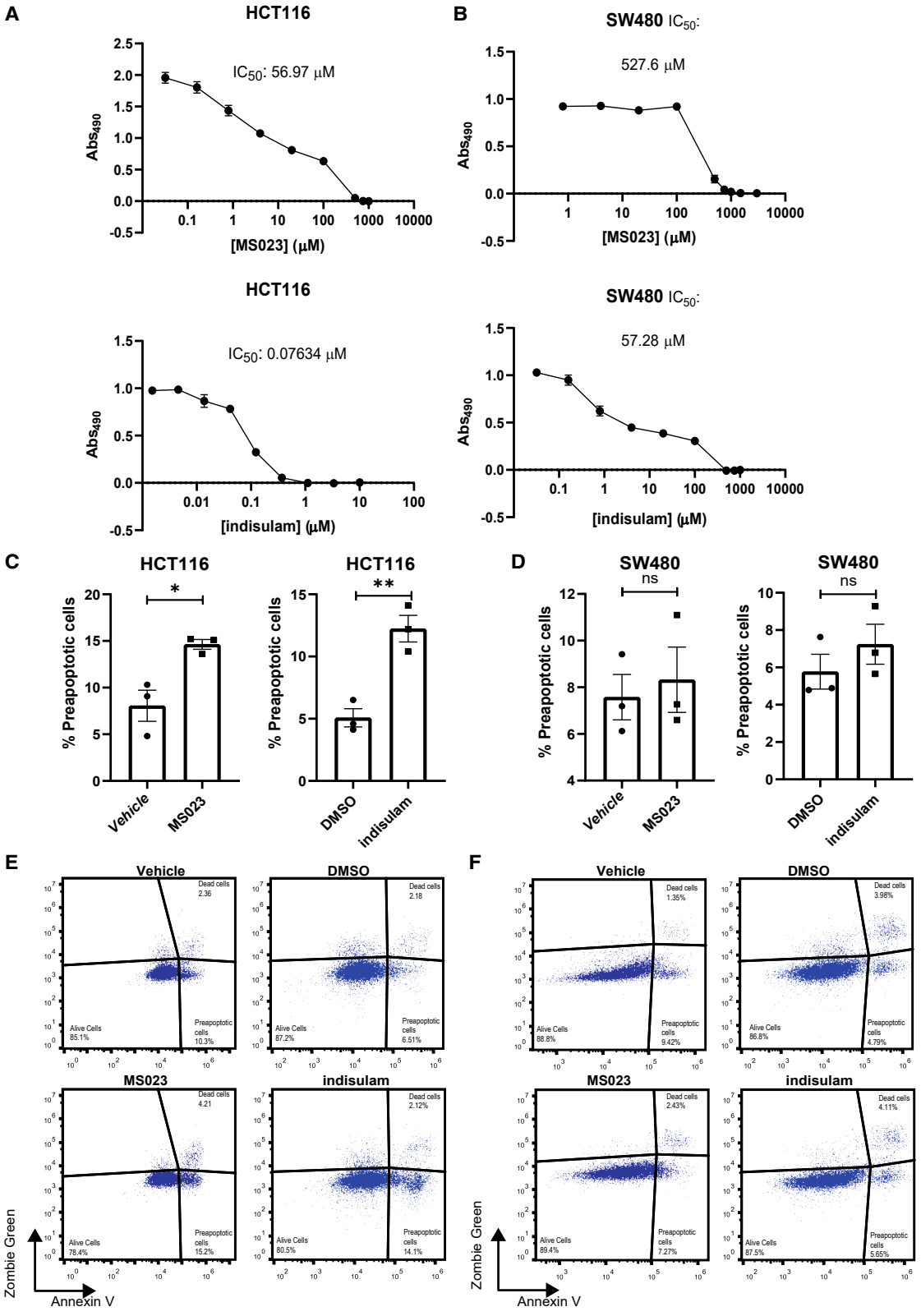

(legend on next page)

mutations harboring PTCs.[14,16,19,25,33] NMD inhibition has been previously linked to increased tumor immunogenicity,[12] and SMG1 itself has emerged as a potential biomarker of response to immune-checkpoint blockade (ICB) therapies.[11,25] Tumors with low SMG1 expression exhibit impaired NMD activity, allowing accumulation of highly immunogenic peptides with strong MHC-binding affinity.[11,25]

In this context, efforts to directly target NMD with small molecules are gaining traction for immunotherapy purposes.[19,29,34,35] Our data unexpectedly reveal that drugs originally developed to modulate splicing may function as indirect yet potent NMD inhibitors. This expands the therapeutic relevance of these agents, positioning them as attractive candidates to augment tumor immunogenicity by dual mechanisms: inducing aberrant splicing-derived antigens and stabilizing otherwise degraded neoepitopes that are under NMD surveillance.

An important unanswered question is which neoantigens, those derived from altered splicing or those normally suppressed by NMD, are more immunodominant. The answer will likely depend on tumor type, mutational background, and immune context. This consideration will be critical in the rational design of neoantigen-based cancer vaccines aiming to include universal cryptic peptides.

Importantly, this strategy may be particularly valuable in tumors with low mutational burden, such as myelodysplastic syndromes (MDSs) and hematological malignancies, where classical mutational neoantigens are scarce.[16,36] Several approaches have been proposed to modulate splicing in cancer, with small-molecule modulators.[18,37,38] In our study, we employed MS023,[18,22,39] an inhibitor of type I PRMTs, and indisulam, a sulfonamide that promotes degradation of the splicing factor RBM39, both of which resulted in NMD suppression through SMG1 impairment. Although we cannot conclude that all splicing perturbations will exert the same effect, it is likely that splicing-targeting drugs interfering with SRSF1, SRSF2, or RBM39 (including other sulfonamides[24] or inhibitors of type I PRMTs) may produce similar outcomes. In our correlation analysis with SMG1, we also included additional splicing factors that are commonly affected by splicing modulators, such as those targeted by CLK inhibitors that alter SRSF phosphorylation.[40] These factors could potentially influence SMG1 expression or activity. However, further studies will be required to systematically evaluate the specific impact of each splicing inhibitor on SMG1.

Pharmacological modulation of splicing can impact multiple genes beyond SMG1, including those essential for normal cellular homeostasis, potentially leading to undesirable side effects. However, cancer cells typically harbor extensive genetic and transcriptomic alterations, which may render them more vulnerable to splicing perturbation than healthy tissues. This differential sensitivity could, at least in part, widen the therapeutic window of these compounds. Importantly, several splicing modulators such as indisulam have already been evaluated in clinical trials[20,41] and demonstrated acceptable tolerability at the doses used. Based on our findings and others,[7] it may be valuable to reanalyze or stratify patient responses in these studies according to MSI status, as MSI tumors—characterized by high genomic instability—are likely to be particularly sensitive to this mechanism. In future work, therapeutic selectivity could be further improved through the development of targeted delivery strategies, such as antibody-drug or aptamer-drug conjugates,[42,43] which would preferentially direct splicing modulators to tumor cells while minimizing systemic exposure.

From a translational standpoint, our results suggest that pharmacological modulation of splicing represents a promising therapeutic approach to enhance tumor immunogenicity and to target tumors that rely on high NMD activity for survival (“NMD-addicted” tumors). However, as splicing and NMD are fundamental processes in normal cells, systemic inhibition could potentially result in adverse effects. Therefore, clinical translation will likely require the development of strategies to maximize tumor selectivity and minimize toxicity. Several approaches could be envisioned: (1) targeted delivery systems, such as antibody-drug conjugates (ADCs) or aptamer-drug conjugates, could direct splicing modulators specifically to tumor cells, reducing systemic exposure and off-target effects[42,43]; (2) biomarker-based patient stratification, identifying tumors with high NMD dependency (e.g., MSI or highly aneuploid tumors) may help to select patients most likely to respond at lower doses[7,8]; and (3) optimized dosing regimens, including intermittent or metronomic schedules, could balance efficacy with safety by leveraging tumor-specific vulnerabilities while allowing normal tissue recovery. Collectively, these translational strategies could enhance the therapeutic window and accelerate clinical development of splicing modulators or NMD-targeting combinations in cancer immunotherapy.

Furthermore, we disclose that SMG1 expression is tightly correlated with the expression of key splicing regulators targeted by these compounds, such as RBM39, SRSF1, and SRSF2, as shown in scRNAseq datasets from multiple tumor types. Downregulation of these splicing factors has been associated with improved antitumor immune responses,[44] possibly due in part to concomitant NMD suppression. Notably, overexpression of SRSF2 has been shown to enhance NMD efficiency,[45,46] and its cancer-associated P95H mutation that provides higher binding to mRNA stabilizing the exon junction complex (EJC), frequently found in MDS, further boosts NMD activity.[47]

Finally, in line with our observation a recent CRISPR-Cas9 screen identified multiple splicing factors whose knockout reduces NMD activity, reinforcing the concept that splicing and

Figure 4. Microsatellite instability sensibilizes to splicing modulators

HCT116 (A) and SW480 (B) were incubated with different MS023 or indisulam concentrations. After 96 h, cell viability was measured by MTS. HCT116 (C) and SW480 (D) colon cell lines were incubated with 100 μM of MS023 or 1 μM of indisulam for 72 h. Then, apoptosis status (Annexin V) and cell viability (Zombie Green) were measured by flow cytometry ($n = 3$ per group). Representative dot plot of HCT116 (E) and SW480 (F) cells treated with 100 μM of MS023 or 1 μM of indisulam (8.000 events). Statistical analysis: unpaired two-tailed Student’s t test was employed in (C) and (D). Data represented as means ± SEM. ns, not significant; $^{*}p < 0.05$, $^{**}p < 0.01$, $^{***}p < 0.001$, $^{****}p < 0.0001$.

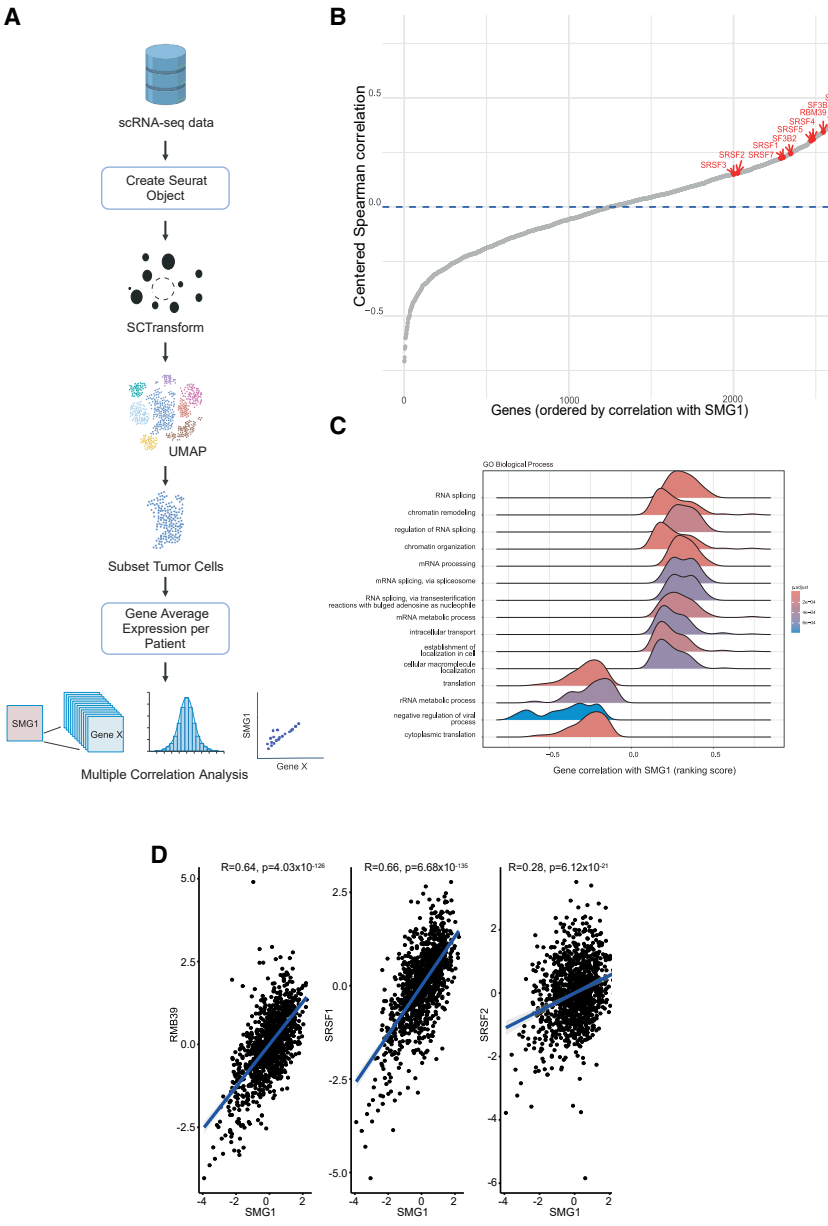

Figure 5. SMG1 expression correlates with genes targeted by splicing-modulating drugs in breast tumor samples

(A) Workflow of single-cell RNA-seq (scRNA-seq) data analysis to establish associations between SMG1 expression and other genes in tumor cells from individual patients in the breast cancer dataset.[30]

(B) Ranking of Spearman correlation values between SMG1 and all transcripts in the tumor cell population. Splicing factors are highlighted in red: SF3B1, SF3B2, SF3B3, SRSF1, SRSF2, SRSF3, SRSF4, SRSF5, SRSF6, SRSF7, RBM39, SF1.

(C) Gene Set Enrichment Analysis (GSEA) of the top GO Biological Process pathways associated with SMG1 expression in tumor samples.

(D) Spearman correlation analysis of SMG1 expression with RBM39, SRSF1, and SRSF2 in RNA-seq data for breast cancer were obtained from The Cancer Genome Atlas (TCGA) from the Genomic Data Commons (GDC) portal.

NMD are functionally intertwined.[48] Collectively, our findings provide mechanistic insight into how splicing modulation inadvertently impacts the NMD pathway and suggest that pharmacological perturbation of splicing could be repurposed as a strategy to enhance antitumor immunity by functionally disabling NMD, and to sensitize MSI tumors that are dependent on NMD.[7]

Limitations of the study

This study has some limitations. First, although our data indicate that splicing modulation suppresses NMD and enhances tumor immunogenicity, we did not perform a comprehensive analysis of the MHC-I peptidome/ligandome to distinguish the relative contribution of NMD blockade versus drug-induced splicing-derived neoantigens elicited by MS023 or indisulam. Such analyses would be necessary to quantify the specific immunopeptidomic impact of each mechanism. Second, our mechanistic investigation focused primarily on the effect of splicing modulation on the NMD kinase SMG1, particularly through intron 29 retention. However, additional NMD components may also be affected—either directly or indirectly—and alternative pathways might contribute to the overall reduction in NMD activity. Finally, we did not assess whether the genetic inhibition of individual splicing factors recapitulates the NMD-suppressive effects observed with pharmacological splicing modulation. However, previous work has already shown that CRISPR-mediated inhibition of multiple splicing factors can lead to NMD blockade,[48] supporting the concept that splicing perturbation and NMD suppression are mechanistically linked.

RESOURCE AVAILABILITY

Lead contact

For further information, requests for resources, or reagents, please contact the lead author, Fernando Pastor (fpasrodri@unav.es), who will handle and fulfill such requests.

Materials availability

All plasmids, cell lines, and mouse models used in this study will be made available upon reasonable request and completion of a material transfer agreement with the corresponding author.

Data and code availability

- This paper analyzes existing, publicly available data (see "deposited data" in the key resources table in STAR Methods).
- This paper does not report original code.
- Any additional information will be available from lead contact upon request.

ACKNOWLEDGMENTS

We are indebted to Elisabet Guruceaga for bioinformatic assistance. This work was supported by Instituto de Salud Carlos III y Fondos Feder (PI23/01120), Asociación Española Contra el Cáncer (AECC PRYES235096PAST), and Gobierno de Navarra Estratégicos "REVOLUTION" (0011-1411-2024-000110).

AUTHOR CONTRIBUTIONS

Conception and design, F.P.; methodology development, all authors; data acquisition: all authors; data analysis and interpretation (including statistical, bioinformatic, and computational analyses), all authors; manuscript writing, review, and editing, M.B. and F.P.; administrative, technical, and material support (including data organization and database construction), all authors; and study supervision, F.P.

DECLARATION OF INTERESTS

The authors declare no competing interests.

DECLARATION OF GENERATIVE AI AND AI-ASSISTED TECHNOLOGIES IN THE WRITING PROCESS

During the preparation of this work, the authors used ChatGPT from OpenAI to improve language and readability. After using this tool, the authors reviewed and edited the content as needed and they take full responsibility for the content of the publication.

STAR★METHODS

Detailed methods are provided in the online version of this paper and include the following:

- KEY RESOURCES TABLE
- EXPERIMENTAL MODEL AND STUDY PARTICIPANT DETAILS
  - Mice strains
  - Cell lines and culture conditions
- METHOD DETAILS
  - Tumor models
  - MTS assay
  - Tumor infiltrate studies by flow cytometry
  - ELISPOT
  - RNA extraction and qRT-PCR
  - Western Blot
  - NMD reporter system
  - Cell viability by flow cytometry
  - RNAseq analysis
- QUANTIFICATION AND STATISTICAL ANALYSIS

SUPPLEMENTAL INFORMATION

Supplemental information can be found online at https://doi.org/10.1016/j.isci.2025.114597.

Received: December 5, 2025
Revised: December 16, 2025
Accepted: December 29, 2025
Published: January 6, 2026

REFERENCES

1. Lykke-Andersen, S., and Jensen, T.H. (2015). Nonsense-mediated mRNA decay: an intricate machinery that shapes transcriptomes. Nat. Rev. Mol. Cell Biol. *16*, 665–677. https://doi.org/10.1038/nrm4063.
2. Kurosaki, T., Popp, M.W., and Maquat, L.E. (2019). Quality and quantity control of gene expression by nonsense-mediated mRNA decay. Nat. Rev. Mol. Cell Biol. *20*, 406–420. https://doi.org/10.1038/s41580-019-0126-2.
3. Nogueira, G., Fernandes, R., García-Moreno, J.F., and Romão, L. (2021). Nonsense-mediated RNA decay and its bipolar function in cancer. Mol. Cancer *20*, 72. https://doi.org/10.1186/S12943-021-01364-0.
4. Bongiorno, R., Colombo, M.P., and Lecis, D. (2021). Deciphering the nonsense-mediated mRNA decay pathway to ixdentify cancer cell vulnerabilities for effective cancer therapy. J. Exp. Clin. Cancer Res. *40*, 376. https://doi.org/10.1186/S13046-021-02192-2.
5. Tan, K., Stupack, D.G., and Wilkinson, M.F. (2022). Nonsense-mediated RNA decay: an emerging modulator of malignancy. Nat. Rev. Cancer *22*, 437–451. https://doi.org/10.1038/s41568-022-00481-2.
6. Nagar, P., Islam, M.R., and Rahman, M.A. (2023). Nonsense-Mediated mRNA Decay as a Mediator of Tumorigenesis. Genes *14*, 357. https://doi.org/10.3390/genes14020357.
7. Bokhari, A., Jonchere, V., Lagrange, A., Bertrand, R., Svrcek, M., Marisa, L., Buhard, O., Greene, M., Demidova, A., Jia, J., et al. (2018). Targeting nonsense-mediated mRNA decay in colorectal cancers with microsatellite instability. Oncogenesis *7*, 70. https://doi.org/10.1038/s41389-018-0079-x.
8. Ippolito, M.R., Zerbib, J., Eliezer, Y., Reuveni, E., Viganò, S., De Feudis, G., Shulman, E.D., Savir Kadmon, A., Slutsky, R., Chang, T., et al. (2024). Increased RNA and Protein Degradation Is Required for Counteracting Transcriptional Burden and Proteotoxic Stress in Human Aneuploid Cells. Cancer Discov. *14*, 2532–2553. https://doi.org/10.1158/2159-8290.CD-23-0309.
9. Bakhoum, S.F. (2024). Targeting RNA and Protein Turnover in Aneuploid Cancers. Cancer Discov. *14*, 2315–2316. https://doi.org/10.1158/2159-8290.CD-24-1350.
10. Lindeboom, R.G.H., Vermeulen, M., Lehner, B., and Supek, F. (2019). The impact of nonsense-mediated mRNA decay on genetic disease, gene editing and cancer immunotherapy. Nat. Genet. *51*, 1645–1651. https://doi.org/10.1038/s41588-019-0517-5.
11. Meraviglia-Crivelli, D., Villanueva, H., Zheleva, A., Villalba-Esparza, M., Moreno, B., Menon, A.P., Calvo, A., Cebollero, J., Barainka, M., de los Mozos, I.R., et al. (2022). IL-6/STAT3 signaling in tumor cells restricts the expression of frameshift-derived neoantigens by SMG1 induction. Mol. Cancer *21*, 211. https://doi.org/10.1186/s12943-022-01679-6.
12. Pastor, F., Kolonias, D., Giangrande, P.H., and Gilboa, E. (2010). Induction of tumour immunity by targeted inhibition of nonsense-mediated mRNA decay. Nature *465*, 227–230. https://doi.org/10.1038/nature08999.
13. Turajlic, S., Litchfield, K., Xu, H., Rosenthal, R., McGranahan, N., Reading, J.L., Wong, Y.N.S., Rowan, A., Kanu, N., Al Bakir, M., et al. (2017). Insertion-and-deletion-derived tumour-specific neoantigens and the immunogenic phenotype: a pan-cancer analysis. Lancet Oncol. *18*, 1009–1021. https://doi.org/10.1016/S1470-2045(17)30516-8.
14. Xie, N., Shen, G., Gao, W., Huang, Z., Huang, C., and Fu, L. (2023). Neoantigens: promising targets for cancer therapy. Signal Transduct. Target. Ther. *8*, 9. https://doi.org/10.1038/s41392-022-01270-x.
15. Jayasinghe, R.G., Cao, S., Gao, Q., Wendl, M.C., Vo, N.S., Reynolds, S.M., Zhao, Y., Climente-González, H., Chai, S., Wang, F., et al. (2018). Systematic Analysis of Splice-Site-Creating Mutations in Cancer. Cell Rep. *23*, 270–281.e3. https://doi.org/10.1016/j.celrep.2018.03.052.
16. Rosenberg-Mogilevsky, A., Siegfried, Z., and Karni, R. (2025). Generation of tumor neoantigens by RNA splicing perturbation. Trends Cancer *11*, 12–24. https://doi.org/10.1016/j.trecan.2024.10.008.

17. Kahles, A., Lehmann, K.-V., Toussaint, N.C., Hüser, M., Stark, S.G., Sachsenberg, T., Stegle, O., Kohlbacher, O., Sander, C., Rätsch, G., et al. (2018). Comprehensive Analysis of Alternative Splicing Across Tumors from 8,705 Patients. Cancer Cell *34*, 211–224.e6. https://doi.org/10.1016/j.ccell.2018.07.001.

18. Lu, S.X., De Neef, E., Thomas, J.D., Sabio, E., Rousseau, B., Gigoux, M., Knorr, D.A., Greenbaum, B., Elhanati, Y., Hogg, S.J., et al. (2021). Pharmacologic modulation of RNA splicing enhances anti-tumor immunity. Cell *184*, 4032–4047.e31. https://doi.org/10.1016/j.cell.2021.05.038.

19. Cook, A.L., Sur, S., Dobbyn, L., Watson, E., Cohen, J.D., Ptak, B., Lee, B. S., Paul, S., Hsiue, E., Popoli, M., et al. (2024). Identification of nonsense-mediated decay inhibitors that alter the tumor immune landscape. eLife *13*, e95952. https://doi.org/10.7554/eLife.95952.1.

20. Assi, R., Kantarjian, H.M., Kadia, T.M., Pemmaraju, N., Jabbour, E., Jain, N., Daver, N., Estrov, Z., Uehara, T., Owa, T., et al. (2018). Final results of a phase 2, open-label study of indisulam, idarubicin, and cytarabine in patients with relapsed or refractory acute myeloid leukemia and high-risk myelodysplastic syndrome. Cancer *124*, 2758–2765. https://doi.org/10.1002/cncr.31398.

21. Eram, M.S., Shen, Y., Szewczyk, M., Wu, H., Senisterra, G., Li, F., Butler, K.V., Kaniskan, H.Ü., Speed, B.A., dela Seña, C., et al. (2016). A Potent, Selective, and Cell-Active Inhibitor of Human Type I Protein Arginine Methyltransferases. ACS Chem. Biol. *11*, 772–781. https://doi.org/10.1021/acschembio.5b00839.

22. Fong, J.Y., Pignata, L., Goy, P.A., Kawabata, K.C., Lee, S.C.W., Koh, C. M., Musiani, D., Massignani, E., Kotini, A.G., Penson, A., et al. (2019). Therapeutic Targeting of RNA Splicing Catalysis through Inhibition of Protein Arginine Methylation. Cancer Cell *36*, 194–209.e9. https://doi.org/10.1016/j.ccell.2019.07.003.

23. Li, W.J., Huang, Y., Lin, Y.A., Zhang, B.D., Li, M.-Y., Zou, Y.Q., Hu, G.S., He, Y.H., Yang, J.J., Xie, B.L., et al. (2023). Targeting PRMT1-mediated SRSF1 methylation to suppress oncogenic exon inclusion events and breast tumorigenesis. Cell Rep. *42*, 113385. https://doi.org/10.1016/j.celrep.2023.113385.

24. Han, T., Goralski, M., Gaskill, N., Capota, E., Kim, J., Ting, T.C., Xie, Y., Williams, N.S., and Nijhawan, D. (2017). Anticancer sulfonamides target splicing by inducing RBM39 degradation via recruitment to DCAF15. Science *356*, eaal3755. https://doi.org/10.1126/science.aal3755.

25. Vendramin, R., Fu, H., Zhao, Y., Fernandez, S., Qian, D., Ligammari, L., Levy, R., Greenberg, P., Castro, A., Thakkar, K., et al. (2024). Pharmacologic inhibition of nonsense-mediated decay induces anti-tumour immunogenicity in ex vivo patient tumours. Sneak Peek *9*, 65. https://doi.org/10.2139/ssrn.4722051.

26. Supek, F., Lehner, B., and Lindeboom, R.G.H. (2021). To NMD or Not To NMD: Nonsense-Mediated mRNA Decay in Cancer and Other Genetic Diseases. Trends Genet. *37*, 657–668. https://doi.org/10.1016/j.tig.2020.11.002.

27. Pimentel, H., Bray, N.L., Puente, S., Melsted, P., and Pachter, L. (2017). Differential analysis of RNA-seq incorporating quantification uncertainty. Nat. Methods *14*, 687–690. https://doi.org/10.1038/nmeth.4324.

28. Huang, L., Lou, C.H., Chan, W., Shum, E.Y., Shao, A., Stone, E., Karam, R., Song, H.W., and Wilkinson, M.F. (2011). RNA homeostasis governed by cell type-specific and branched feedback loops acting on NMD. Mol. Cell *43*, 950–961. https://doi.org/10.1016/j.molcel.2011.06.031.

29. Langer, L.M., Bonneau, F., Gat, Y., and Conti, E. (2021). Cryo-EM reconstructions of inhibitor-bound SMG1 kinase reveal an autoinhibitory state dependent on SMG8. eLife *10*, e72353. https://doi.org/10.7554/eLife.72353.

30. Bassez, A., Vos, H., Van Dyck, L., Floris, G., Arijs, I., Desmedt, C., Boeckx, B., Vanden Bempt, M., Nevelsteen, I., Lambein, K., et al. (2021). A single-cell map of intratumoral changes during anti-PD1 treatment of patients with breast cancer. Nat. Med. *27*, 820–832. https://doi.org/10.1038/s41591-021-01323-8.

31. Hafemeister, C., and Satija, R. (2019). Normalization and variance stabilization of single-cell RNA-seq data using regularized negative binomial regression. Genome Biol. *20*, 296. https://doi.org/10.1186/s13059-019-1874-1.

32. Jerby-Arnon, L., Shah, P., Cuoco, M.S., Rodman, C., Su, M.J., Melms, J.C., Leeson, R., Kanodia, A., Mei, S., Lin, J.R., et al. (2018). A Cancer Cell Program Promotes T Cell Exclusion and Resistance to Checkpoint Blockade. Cell *175*, 984–997.e24. https://doi.org/10.1016/J.CELL.2018.09.006.

33. Becker, J.P., Helm, D., Rettel, M., Stein, F., Hernandez-Sanchez, A., Urban, K., Gebert, J., Kloor, M., Neu-Yilik, G., von Knebel Doeberitz, M., et al. (2021). NMD inhibition by 5-azacytidine augments presentation of immunogenic frameshift-derived neoepitopes. iScience *24*, 102389. https://doi.org/10.1016/j.isci.2021.102389.

34. Meraviglia-Crivelli, D., Villanueva, H., Menon, A.P., Zheleva, A., Moreno, B., Villalba-Esparza, M., and Pastor, F. (2022). A pan-tumor-siRNA aptamer chimera to block nonsense-mediated mRNA decay inflames and suppresses tumor progression. Mol. Ther. Nucleic Acids *29*, 413–425. https://doi.org/10.1016/j.omtn.2022.07.017.

35. Zhang, Y., Xie, X., Yeganeh, P.N., Lee, D.J., Valle-Garcia, D., Meza-Sosa, K.F., Junqueira, C., Su, J., Luo, H.R., Hide, W., et al. (2021). Immunotherapy for breast cancer using EpCAM aptamer tumor-targeted gene knockdown. Proc. Natl. Acad. Sci. USA *118*, e2022830118. https://doi.org/10.1073/PNAS.2022830118.

36. Roerden, M., Nelde, A., and Walz, J.S. (2019). Neoantigens in Hematological Malignancies—Ultimate Targets for Immunotherapy? Front. Immunol. *10*, 3004. https://doi.org/10.3389/fimmu.2019.03004.

37. Bowling, E.A., Wang, J.H., Gong, F., Wu, W., Neill, N.J., Kim, I.S., Tyagi, S., Orellana, M., Kurley, S.J., Dominguez-Vidaña, R., et al. (2021). Spliceosome-targeted therapies trigger an antiviral immune response in triple-negative breast cancer. Cell *184*, 384–403.e21. https://doi.org/10.1016/j.cell.2020.12.031.

38. Matsushima, S., Ajiro, M., Iida, K., Chamoto, K., Honjo, T., and Hagiwara, M. (2022). Chemical induction of splice-neoantigens attenuates tumor growth in a preclinical model of colorectal cancer. Sci. Transl. Med. *14*, eabn6056. https://doi.org/10.1126/scitranslmed.abn6056.

39. Maron, M.I., Casill, A.D., Gupta, V., Roth, J.S., Sidoli, S., Query, C.C., Gamble, M.J., and Shechter, D. (2022). Type I and II PRMTs inversely regulate post-transcriptional intron detention through Sm and CHTOP methylation. eLife *11*, e72867. https://doi.org/10.7554/eLife.72867.

40. Song, M., Pang, L., Zhang, M., Qu, Y., Laster, K.V., and Dong, Z. (2023). Cdc2-like kinases: structure, biological function and therapeutic targets for diseases. Signal Transduct. Target. Ther. *8*, 148. https://doi.org/10.1038/s41392-023-01409-4.

41. Talbot, D.C., von Pawel, J., Cattell, E., Yule, S.M., Johnston, C., Zandvliet, A.S., Huitema, A.D.R., Norbury, C.J., Ellis, P., Bosquee, L., et al. (2007). A Randomized Phase II Pharmacokinetic and Pharmacodynamic Study of Indisulam as Second-Line Therapy in Patients with Advanced Non–Small Cell Lung Cancer. Clin. Cancer Res. *13*, 1816–1822. https://doi.org/10.1158/1078-0432.CCR-06-0249.

42. Tsuchikama, K., Anami, Y., Ha, S.Y.Y., and Yamazaki, C.M. (2024). Exploring the next generation of antibody–drug conjugates. Nat. Rev. Clin. Oncol. *21*, 203–223. https://doi.org/10.1038/s41571-023-00850-2.

43. Su, M., Liu, Y., Lin, H., Wang, X., Ying, D., Zhang, L., Yang, C., Jiang, M., Xu, L., Wang, X., et al. (2025). An aptamer-drug conjugate for promising cancer therapy with comprehensive evaluation from rodents to non-human primates. Signal Transduct. Target. Ther. *10*, 316. https://doi.org/10.1038/s41392-025-02399-1.

44. Kim, W.J., Crosse, E.I., De Neef, E., Etxeberria, I., Sabio, E.Y., Wang, E., Bewersdorf, J.P., Lin, K.-T., Lu, S.X., Belleville, A., et al. (2025). Mis-splicing-derived neoantigens and cognate TCRs in splicing factor mutant leukemias. Cell *188*, 3422–3440.e24. https://doi.org/10.1016/j.cell.2025.03.047.

45. Zhang, Z., and Krainer, A.R. (2004). Involvement of SR Proteins in mRNA Surveillance. Mol. Cell *16*, 597–607. https://doi.org/10.1016/j.molcel.2004.10.031.

46. Aznarez, I., Nomakuchi, T.T., Tetenbaum-Novatt, J., Rahman, M.A., Fregoso, O., Rees, H., and Krainer, A.R. (2018). Mechanism of Nonsense-Mediated mRNA Decay Stimulation by Splicing Factor SRSF1. Cell Rep. *23*, 2186–2198. https://doi.org/10.1016/j.celrep.2018.04.039.

47. Rahman, M.A., Lin, K.-T., Bradley, R.K., Abdel-Wahab, O., and Krainer, A.R. (2020). Recurrent SRSF2 mutations in MDS affect both splicing and NMD. Genes Dev. *34*, 413–427. https://doi.org/10.1101/gad.332270.119.

48. Cheruiyot, A., Li, S., Nonavinkere Srivatsan, S., Ahmed, T., Chen, Y., Lemacon, D.S., Li, Y., Yang, Z., Wadugu, B.A., Warner, W.A., et al. (2021). Nonsense-mediated RNA Decay Is a Unique Vulnerability of Cancer Cells harboring SF3B1 or U2AF1 mutations. Cancer Res. *81*, 4499–4513. https://doi.org/10.1158/0008-5472.CAN-20-4016.

49. Bolger, A.M., Lohse, M., and Bjoem, U. (2014). Trimmomatic: a flexible trimmer for Illumina sequence data. Bioinformatics *30*, 2114–2120. https://doi.org/10.1093/bioinformatics/btu170.

50. Bray, N.L., Pimentel, H., Melsted, P., and Pachter, L. (2016). Near-optimal probabilistic RNA-seq quantification. Nat. Biotechnol. *34*, 525–527. https://doi.org/10.1038/nbt.3519.

STAR★METHODS

KEY RESOURCES TABLE

REAGENT or RESOURCE	SOURCE	IDENTIFIER
Antibodies		
PerCP/Cyanine5.5 anti-mouse CD45	BioLegend	Cat#103131, RRID:AB_893344
APC/Fire 750 anti-mouse CD8a	BioLegend	Cat#100765, RRID:AB_2572112
Brilliant Violet 510 anti-mouse CD4	BioLegend	Cat#100449, RRID:AB_2564587
APC anti-mouse CD25	BioLegend	Cat#102012, RRID:AB_312861
Alexa Fluor 700 anti-mouse/human CD11b	BioLegend	Cat#101222, RRID:AB_493705
Brilliant Violet 421 anti-mouse CD11c	BioLegend	Cat#117329, RRID:AB_10897814
PE/Cyanine7 anti-mouse F4/80	BioLegend	Cat#123113, RRID:AB_893490
PE anti-FOXP3 (FJK-16s)	ThermoFisher Scientific	Cat#12-5773-82, RRID:AB_465936
Annexin V Recom APC	BD Biosciences	Cat# 550475; RRID:AB_2868885
Anti-SMG1 (Q25) Rabbit Ab	Cell Signaling	Cat#4993; RRID:AB_2192938
Anti-β-Actin (13E5) Rabbit Ab	Cell Signaling	Cat#4970; RRID:AB_2223172
Anti-Vinculin (E1E9V) Rabbit Ab	Cell Signaling	Cat#13901; RRID:AB_2728768
Anti-rabbit IgG, HRP-linked Antibody	Cell Signaling	Cat#7074; RRID:AB_2099233
Chemicals, peptides, and recombinant proteins		
PBS	Gibco	Cat#14190144
Trypsin-EDTA (0.05%)	Gibco	Cat#25300054
RPMI-1640	Gibco	Cat#21875034
Dulbecco's modified Eagle's medium (DMEM)	Gibco	Cat#41966052
McCoy HyClone 5A	Cytiva	Cat#SH30200.01
Fetal Bovine Serum	Gibco	Cat#A5256701
L-Glutamine	Gibco	Cat#25030024
Penicillin-Streptomycin	Gibco	Cat#15140122
Sodium Pyruvate	Gibco	Cat#11360070
β-mercaptoethanol (2-mercaptoethanol)	MilliporeSigma	Cat#21985023
HEPES	Gibco	Cat#15630080
MEM Non-Essential Amino Acids Solution	Gibco	Cat#11350912
MS023	Tocris	Cat#5713
Indisulam	MilliporeSigma	Cat#SML1225-25 MG
SMG1i (hSMG-1 inhibitor 11j)	MedchemExpress	Cat#HY-124719
1-methyl-2-pyrrolidinone	MilliporeSigma	Cat#494496-1L
Captisol (SBE-b-CD (Synonyms: Sulfobutylether-b-Cyclodextrin)	SelleckChem	Cat#182410-00-0
Polyethylene glycol 400	MilliporeSigma	Cat#91893-1L-F
DMSO	WAK-Chemie Medical GmbH	Cat#WAK-DMSO-10
Collagenase D	Roche	Cat#11088858001
Recombinant DNase I	Roche	Cat#4536282001
EDTA	Invitrogen	Cat#15575020
ACK Lysis buffer	Gibco	Cat#A10492-01
BSA	MilliporeSigma	Cat#A9647
Triton X-100	MilliporeSigma	Cat#X-100
cOmplete™ Protease Inhibitor Cocktail	Roche	Cat#04693116001
Bovine Serum Albumin Standard Ampules, 2 mg/mL	ThermoFisher Scientific	Cat#23209

(*Continued on next page*)

Continued

REAGENT or RESOURCE	SOURCE	IDENTIFIER
NuPAGE™ LDS Sample Buffer (4X)	Invitrogen	Cat#NP0007
HiMark™ Pre-stained Protein Standard	Invitrogen	Cat#LC5699
Bio-Rad 10x Tris/Glycine/SDS Buffer 5 L	Bio-Rad	Cat#1610772
10x Tris/Glycine Buffer 5L	Bio-Rad	Cat#1610771
10x Tris-Buffered Saline (TBS)	Bio-Rad	Cat#1706435
Methanol	PanReac AplliChem	Cat#141091.1211
Ethanol	PanReac AplliChem	Cat#361086.1611
Tween 20	MilliporeSigma	Cat#P9416
GeneAmp dNTP Blend 100 mM	Applied Biosystems	Cat#N8080261
Random Hexamers 50 μM	Invitrogen	Cat#N8080127
RNaseOUT™ Recombinant Ribonuclease Inhibitor	Invitrogen	Cat#10777019
NaCl	MilliporeSigma	Cat#59888
$CaCl_2$	MilliporeSigma	Cat#C1016
Critical commercial assays		
MycoAlert™ PLUS Mycoplasma Detection Kit	Lonza	Cat#LT07-710
CellTiter 96® AQ_{ueous} One Solution Cell Proliferation Assay (MTS)	Promega	Cat#G3581
eBioscience™ Foxp3/Transcription Factor Staining Buffer Set	Invitrogen	Cat#00-5523-00
Cytofix/Cytoperm™ Fixation/ Permeabilization Kit	BD Biosciences	Cat#554714; RRID:AB_2869008
ELISPOT Mouse IFNg ELISPOT Set	BD Biosciences	Cat#551083; RRID:AB_2868922
Bio-Rad Protein Assay Dye Reagent Concentrate	Bio-Rad	Cat#5000006
4–15% Mini-PROTEAN® TGX™ Precast Protein Gels	Bio-Rad	Cat#4561084
Nitrocellulose Membrane, Roll, 0.45 μm	Bio-Rad	Cat#1620115
ECL™ Western Blotting Detection Reagents	Cytiva	Cat#RPN2209
ECL™ Prime Western Blotting Detection Reagent	Cytiva	Cat#RPN2236
RNeasy Mini Kit	Qiagen	Cat#74104
M-MLV Reverse Transcriptase	Invitrogen	Cat#28025021
Fast SYBR™ Green Master Mix	Applied Biosystems	Cat#4385612
ONE-Glo™ Luciferase Assay System	Promega	Cat#E6120
Zombie Green™ Fixable Viability Kit	BioLegend	Cat#423111
Deposited data		
BRCA scRNAseq data	lambrechtslab	https://lambrechtslab.sites.vib.be/en/single-cell
Melanoma scRNAseq data	NCBI Gene Expression Omnibus	GSE115978
RNAseq data from three human melanoma cell lines	Lu et al.[18]	N/A
RNA seq data of TCGA	cbioportal	https://www.cbioportal.org/
Experimental models: Cell lines		
Mouse: 4T1 g.Ctrl	Generated in laboratory[11]	N/A
Mouse: 4T1 $SMG1^{KO}$	Generated in laboratory[11]	N/A
Mouse: B16/F10 g.Ctrl	Generated in laboratory[11]	N/A
Mouse: B16/F10 $SMG1^{KO}$	Generated in laboratory[11]	N/A

(*Continued on next page*)

Continued

REAGENT or RESOURCE	SOURCE	IDENTIFIER
Mouse: Panc02 GS17 WT	Generated in laboratory[11]	N/A
Mouse: Panc02 GS17 PTC	Generated in laboratory[11]	N/A
Human: ARST	N/A	N/A
Human: HCT116	N/A	N/A
Human: SW480	N/A	N/A
Experimental models: Organisms/strains		
Mouse: BALB/c female	Envigo	RRID:MGI:2161072
Mouse: C57BL/6J female	Envigo	RRID:MGI:3028467
Mouse: BALB/c female Rag2$^{-/-}$ IL2Rγ−/−	Bred in house	N/A
Oligonucleotides		
GCCGCTAGAGGTGAAATTC	MilliporeSigma	18s forward
GAAAACATTCTTGGCAAT	MilliporeSigma	18s reverse
GCCATTGGAGAGCTGTCTTC	MilliporeSigma	ATF3 forward
GGGCCATCTGGAACATAAGA	MilliporeSigma	ATF3 reverse
GGGGATTTCCCCACTTTTGAG	MilliporeSigma	SMG1 retained intron forward
ATGACACGCTCTGTGCTAGG	MilliporeSigma	SMG1 retained intron reverse
Recombinant DNA		
pSBbi-Pur	Addgene	Cat#60523
Software and algorithms		
GraphPad Prism	GraphPad Software	V8
FlowJo	BD Biosciences	V10
FastQC	Babraham Bioinformatics	https://www.bioinformatics.babraham.ac.uk/projects/fastqc/
Trimmomatic	Bolger et al.[49]	http://www.usadellab.org/cms/?page=trimmomatic
Kallisto	Bray et al.[50]	https://pachterlab.github.io/kallisto/
R/Bioconductor	Pimentel et al.[27]	https://www.bioconductor.org/
Sleuth package	Pimentel et al.[27]	https://github.com/pachterlab/sleuth
Seurat R package	Seurat	https://satijalab.org/seurat/, V5
R script for Figure 5	N/A	https://github.com/Fpastro/Fig.-5 git

EXPERIMENTAL MODEL AND STUDY PARTICIPANT DETAILS

Mice strains

Balb/c and C57BL/6J mice were purchased from Envigo, and Rag2$^{-/-}$ IL2Rγ$^{-/-}$ mice were bred in-house. All experiments were performed using 6-8 weeks old female mice. Animal studies were approved by the Animal Ethical Committee of the University of Navarra in the veterinary facilities of the Center for Applied Medical Research (CIMA) under the protocol 043-19, following the institutional, national laws and ethical guidelines for experimental animal care.

Cell lines and culture conditions

Panc02 and ARST cell line provided by Dr. I. Melero (CIMA, Pamplona, Spain), 4T1, HCT116 and SW480 cells by Dr. F. Lecanda (CIMA, Pamplona, Spain) and B16/F10 by Dra. S. Hervás-Stubbs (CIMA, Pamplona, Spain). Genetically modified 4T1, Panc02 and B16/F10 cell lines (g.Ctrl/SMG1^{KO} by CRISPR and luciferase NMD reporter plasmid by Sleeping Beauty-based stable transfection) were previously generated in the laboratory.[11]

Cell lines were cultured in RPMI-1640 medium (4T1 and ARST), Dulbecco's modified Eagle's medium (DMEM) (B16/10, Panc02 and SW480) (all from Gibco) or McCoy HyClone 5A medium (Cytiva) (HCT116) supplemented with 8–10% heat-inactivated FBS, 100 U/ml L-glutamine, and 100 μg/mL penicillin/streptomycin (all from Gibco). Lymph node cells medium consisted in RPMI that was additionally supplemented with 1 mM sodium pyruvate (all from Gibco), 0.05 mM β-mercaptoethanol (MilliporeSigma), 1 mM HEPES, and 1× minimal essential medium (MEM) non-essential amino acids (all from Gibco). All cell lines and assay cultures were maintained at 37°C and 5% CO_2. All cells were mycoplasma-free and tested regularly using MycoAlert PLUS Mycoplasma Detection Kit (Lonza).

METHOD DETAILS

Tumor models

Balb/c mice (6-8 weeks old female) were inoculated (subcutaneously) with 5×10^4 4T1 g.Ctrl and SMG1^{KO} breast carcinoma cell, both of which have been previously treated for 96 hours with 5 μM of MS023 or corresponding vehicle. For MS023 (Tocris) dilution, 62.5 mg of MS023 were diluted mixed with 563 mL of 1-methyl-2-pyrrolidinone (MilliporeSigma), 2.257 mL of 20% Captisol in sterile water (w/v, SelleckChem), and 2.257 mg of polyethylene glycol 400 (PEG-400, MilliporeSigma) diluted in 6.21 mL of PBS. Before injecting, the cells were washed 3 times with PBS to remove all drug. 10 mice were inoculated per group, and tumor volumes were measured over time. The same experiment was performed using Rag2$^{-/-}$ IL2Rγ$^{-/-}$ immunodeficient mice.

In a parallel experiment, C57BL/6J (6-8 weeks old female) were inoculated (subcutaneous) with 1.5×10^5 B16/F10 g.Ctrl and SMG1^{KO} breast carcinoma cell pretreated for 96 hours with 1 μM of indisulam (MilliporeSigma) or DMSO. Before injecting, the cells were washed 3 times with PBS to remove all drug. 10 mice were inoculated per group, and tumor volumes were measured over time.

Tumor volume was measured using an electronic caliper. Volume was calculated with the following formula: Tumor volume = [length $\times$ (width)^2]/2.

MTS assay

4T1 g.Ctrl and SMG1^{KO}, and B16/F10 g.Ctrl and SMG1^{KO} were placed in a flat bottom p96-well plate (Falcon) in 50 mL of complete medium. Once cells were attached, 4T1 were treated with 0.004–30 μM of MS023 (in 1:3 serial dilutions) and B16/F10 with 0.2–30 μM of indisulam (in 1:2 serial dilutions) for 96 hours. Each condition was tested three times, and the corresponding vehicle was used as negative control. After 96 hours, the medium was replaced with 100 μL of complete medium with 20 μL of CellTiter 96 AQueous One Solution Cell Proliferation Assay (Promega) and incubated for 30–60 minutes at 37°C and 5% CO_2. Absorbance was measured at 490 nm for each condition using GloMax Discover Microplate Reader (Promega).

HCT116 and SW480 cells' sensitivity to MS023 and indisulam was also tested. HCT116 were cultured with 0.03–1000 μM of MS023 (in 1:5 serial dilution upon 500 μM) and 0.015–10 μM of indisulam (in 1:3 serial dilution). SW480 were cultured with 0.8–3000 μM of MS023 (in 1:5 serial dilution upon 500 μM) and 0.03–1000 μM of indisulam (in 1:5 serial dilution upon 500 μM). Same protocol as for murine 4T1 and B16/F10 cells was followed.

Tumor infiltrate studies by flow cytometry

4T1 cells were treated for 96 hours with MS023 or Vehicle before implantation in Balc/c mice. After 14 days, tumors were resected and placed in Petri dishes (Greiner Bio-One). Tumor mass was measured before digesting with 5 mL of medium containing collagenase D 1 mg/mL and DNase I 0.1 mg/mL (Roche) for 30 minutes at 37°C. Once digested, 100 μL of EDTA (Invitrogen) were added to tumors to stop the digestion. Tumor samples were homogenized and filtered through a 40 μm nylon cell strainer (Falcon) to a 50-mL centrifuge conical tube (Corning). Filtered cells were centrifuged at 1.700 rpm for 5 minutes at room temperature. Supernatant was removed and cells were resuspended in 1 mL of ACK lysis buffer (Gibco) to incubate for 1 minutes in agitation, to lysate erythrocytes. 50 mL of PBS with 2 mM EDTA (Gibco) and 5 mg/ml BSA (MilliporeSigma) were added to stop lysis, and cells were pelleted again at 1.700 rpm for 5 minutes at room temperature. The cells were re-suspended un 200 μL of PBS to move from the tube to a 96-well plate with V-bottom (ThermoFisher), and the plate was centrifuged at 1.700 rpm for 1 minutes at room temperature. Cell pellets were re-suspended in 100 μL of Zombie Green (BioLegend) diluted 1:100 in PBS and then were incubated for 15 minutes at room temperature protected from light. 20 μL of the following antibody mix was added: CD45-PerCP-Cy5.5; CD8a-APC-Fire750; CD4-BV510; CD25-APC; CD11b-AF700; CD11c-BV421; F4/80-PE/Cy7 (all from BioLegend). After 20 minutes at room temperature protected from light, cells were washed twice with PBS and were permeabilized using eBioscience FOXP3/transcription factor buffer set (eBiosciences). Briefly, cells were first resuspended in 200 μL of Foxp3 Fixation/Permeabilization working solution and incubated for 30 minutes protected from light at room temperature. The plate was centrifuged at 1.700 rpm for 1 minutes at room temperature and cells were washed twice with 200 μL of Permeabilization Buffer. Cells were resuspended with 100 μL of Permeabilization Buffer before adding anti-FoxP3-PE antibodies (Invitrogen) and were incubated for 30 minutes at room temperature protected from light for intracellular staining. Then, cells were washed twice with 200 μL of Permeabilization Buffer and fixed with Cytofix/Cytoperm buffer (BD Biosciences) for 10 minutes at 4°C protected from light. Finally, cells were washed twice to remove the remaining paraformaldehyde and samples were acquired using CytoFLEX LS flow cytometer (Beckman Coulter). Data was analyzed using FlowJo 10 (FlowJo). See gating strategy in Figure S2. The percentage of leukocytic populations was calculated relative to total CD45$^+$ live cells and normalized to the processed tumor mass.

ELISPOT

4T1 cells were treated with MS023 and implanted in Balb/c mice as described previously. On day 14, mice were sacrificed and tumor draining lymph nodes were collected for lymphocyte isolation, by homogenizing and filtering through a 40 μm nylon cell strainer (Falcon) to a 50-mL centrifuge conical tube (Corning). Cells were pelleted at 1.700 rpm for 5 minutes at room temperature to be resuspended in Lymph node cells medium (see cell lines and culture conditions section). Then, an IFN-γ ELISPOT (BD Biosciences) assay was performed to quantify reactive T cells against peptides derived from TP53 (NMD dependent): Vehicle or MS023 group lymphocytes were incubated for 24 hours with TP53 (RYPAITSL) at 10 μg/mL in ELISPOT plates previously coated with anti-mouse IFN-γ

antibodies. A similar experiment was performed where tumor draining lymphocytes were incubated with 4T1 g.Ctrl and SMG1^{KO} cells. The plates were revealed and read following manufacturer's instructions. Spots were counted in an ImmunoSpot device.

RNA extraction and qRT-PCR

ARST human cells were cultured in 6-well plates (Falcon) for 96 hours with 5 μM MS023 or 1 μM indisulam, with corresponding vehicle (DMSO for indisulam). After 96 hours, cells were washed with PBS and frozen at −80°C. Then, RNA extraction was performed with the RNeasy Mini Kit (Qiagen). Briefly, cells were lysed with 350 μL of RLT 1% β-mercaptoethanol and then collected in RNeasy Mini Spin Columns with 350 μL of Ethanol 70%. After washing with RW1 buffer, DNA digestion was performed by incubating columns with RNase free DNase diluted in RDD buffer for 15 minutes at room temperature. Then, another wash was performed with RW1 buffer and two additional washes with RPE buffer. RNA was eluted with 30 μL of RNase-free water.

After RNA quantification using NanoDrop, 4.000 μg of RNA were used for cDNA generation, by mixing 4.000 μg in 13 μL RNasa free water with 1 μL of GeneAmp dNTP Blend 100 mM (Applied Biosystems) and 1 μL of Random Hexamer (Invitrogen). The mix was incubated for 5 minutes in 65°C, and, after that, 1 μL of RNase OUT Recombinant Ribonuclease Inhibitor, 1 μL of M-MLV Reverse Transcriptase, 1 μL of 0.1M DTT, and 4 μL 5× First Strand Buffer (all from Invitrogen) were added in order to perform reverse transcriptase PCR in the following conditions: 25°C, 10 minutes; 37°C, 50 minutes; 70°C, 15 minutes. The resulting cDNA was diluted to 100 μg/μL.

For the qRT-PCR, 2 μL of cDNA were mixed with 2.5 μL of Fast SYBR Green Master Mix (Invitrogen) and 1 μL of Primer Set (forward and reverse, both at 10 μM). 3 different primer sets were used (purchased in MilliporeSigma): 18s as housekeeping (Forward 5′GCCGCTAGAGGTGAAATTC, Reverse 5′GAAAACATTCTTGGCAAT), ATF3 (Forward 5′GCCATTGGAGAGCTGTCTTC, Reverse 5′GGGCCATCTGGAACATAAGA), and SMG1 retained intron (Forward 5′GGGGATTTCCCCACTTTTGAG, Reverse 5′ATGACACGCT CTGTGCTAGG). The qRT-PCR was performed using Hard-Shell PCR plates 384 well (Bio-Rad) in QuantStudio 5 Real-Time PCR System.

Western Blot

Tumor cells, previously treated for 96 hours with splicing-altering drugs indisulam and MS023, with the corresponding vehicle as control, were mixed with Lysis Buffer (PBS 1% Triton X-100 (MilliporeSigma) and 20% cOmplete Protease Inhibitor Cocktail (Roche)) and incubated for 30 minutes in ice. Then, protein samples were centrifuged at 10.000 rpm for 15 minutes at 4°C. Supernatant was collected for protein quantification, using Protein Assay Dye Reagent Concentrate (BioRad) diluted in deionized water. 50–100 μg of protein were mixed with 5 μL NuPAGE LDS Sample Buffer 4 × 2.5% β-mercaptoethanol (Invitrogen) in a final volume of 20 μL, which was loaded in BioRad mini-PROTEAN TGX 4–15% gels to run the electrophoresis in 130 V for 90 minutes. HiMark Pre-Stained HMW Protein Standard (Invitrogen) was used as a molecular weight ladder. Then, the proteins were electro-transferred to a 0.45-μm pore size nitrocellulose membrane (BioRad) for 130 V for 75 minutes. The membrane was blocked with 5% milk in TBS-T (TBS BioRad, 0.1% Tween MilliporeSigma) for one hour before adding the primary antibody. The membranes were incubated with rabbit anti-SMG1 (Cell Signaling; 1:1.000; clone Q25), anti-mouse β-Actin (Cell Signaling; 1:2.000; clone 13E5), and anti-human Vinculin (Cell Signaling; 1:1.000; clone E1E9V) overnight at 4°C in agitation. Afterward, once the membranes have been washed three times, HRP-linked anti-rabbit antibody (Cell Signaling; 1:5.000) was used as a secondary antibody. Proteins were detected by chemiluminescence using Amersham ECL Western Blotting Detection Reagents or Amersham ECL Prime Western Blotting Detection Reagents (GE Healthcare) in a ChemiDoc device (BioRad).

NMD reporter system

Two different Panc02 cell lines were used, both with different versions of Sleeping Beauty-based NMD luciferase reporter system.[11] This plasmid consists of the EF-1α pSBbi-Pur (Addgene plasmid #60523) in phase with the firefly luciferase protein (with a PEST motive in the 5′ end to allow protein turnover, to detect protein fluctuations) and the β-globin cassette (Figure 3F). The β-globin cassette contains a nonsense mutation, with a PTC at position 39 that facilitates the degradation by NMD flanked by two introns. The β-globin cassette was cloned downstream the luciferase gene after removing the canonical stop codon. Therefore, the luciferase emission of light of the plasmid bearing a PTC will be dependent on NMD activity. A second version of the plasmid containing the wild-type β-globin sequence was used as a control to normalize luciferase activity from the PTC construct, thereby minimizing variability due to random Sleeping Beauty vector integration and other experimental factors. Both cell lines were generated by transfection and subsequent selection using puromycin. To avoid biases associated with clonal variability—such as differences in integration sites or genetic drift—we worked with pools of selected cells rather than individual clones.

Both Panc02 cells lines were treated with a splicing modulator drug and corresponding vehicle for 48 hours. Cells were washed to remove culture medium and ONE-Glo Luciferase Assay System was added to the cells to lyse them and allow light emission. After incubating the mix for 8 minutes in agitation, RLU for each condition was measured using GloMax Discover Microplate Reader (Promega). The cell line with the wild type β-globin gene RLU was used to normalize the signal of the PTC bearing β-globin gene. As positive control of the NMD reporter plasmid, we performed a similar experiment treating Panc02 cells with SMG1i at 0.3 μM.

Cell viability by flow cytometry

HCT116 and SW480 were placed in 6-well plates (Falcon) and once attached they were treated with 100 μM of MS023, 1 μM of indisulam (and corresponding vehicle), or 0.5 μM of SMG1i. After 72 hours, cells were trypsinized for collection without discarding

culture medium, so as not to lose dead detached cells. After 3 washes with PBS, the cells were resuspended in 200 μL of PBS to move from the tube to 96-well plate with V-bottom (ThermoFisher Scientific), and the plate was centrifuged at 1.900 rpm for 2 min at room temperature. Supernatant was discarded and 100 μL of Zombie Green (diluted 1:200) were added. After incubating 15 minutes at room temperature in darkness, cells were washed with 200 μL of PBS-FBS Buffer (500 mL of PBS supplemented with 2.5 mL of FBS) in order to remove remaining Zombie Green. Then, 100 μL of Binding Buffer (0.01M Hepes, 0.14M NaCl, 2.5 mM $CaCl_2$) was added with 3 μL of Annexin V-APC (BD Biosciences) to each well. After incubating 15 minutes at room temperature in darkness, 300 μL of Binding buffer was added and cells were acquired using DxFlex flow cytometer (Beckman Coulter). Data was analyzed using FlowJo 10 (FlowJo). See gating strategy in Figure S5.

RNAseq analysis

Public RNA sequencing data analysis was performed using the following workflow: (1) the quality of the samples was verified using FastQC software (https://www.bioinformatics.babraham.ac.uk/projects/fastqc/) and the trimming of the reads with trimmomatic (http://www.usadellab.org/cms/?page=trimmomatic); (2) pseudoalignment against the human reference genome (GRCh38) and the quantification of the transcript abundances were performed using kallisto[50] (https://pachterlab.github.io/kallisto/); (3) the transcript annotation reference was Gencode v44; and (4) differential expression statistical analysis was performed using R/Bioconductor (https://www.bioconductor.org/) and sleuth package (https://github.com/pachterlab/sleuth).[27]

After quality assessment and outlier detection using R/Bioconductor, a filtering process was performed. Transcripts with read counts lower than 5 in more than 50% of the samples of all the studied conditions were considered as not expressed in the experiment under study. Transcript expression data were first normalized and then a differential expression analysis between the experimental conditions was performed. Gene expression values represent log2-transformed estimated counts, which have been normalized by Sleuth to account for gene length, sequencing depth, and compositional bias.[27]

BRCA scRNAseq read count data was downloaded from https://lambrechtslab.sites.vib.be/en/single-cell.[30] Melanoma scRNA-seq data was downloaded from the NCBI Gene Expression Omnibus database (accession code GSE115978).[32] Seurat R package was used for analysis (https://satijalab.org/seurat/). Single-cell RNA-seq data were reanalyzed using the Seurat v5 pipeline with SCTransform normalization to correct for technical covariates including total UMI counts, mitochondrial read percentage, and cell cycle phase (S and G2M). After normalization and scaling, Spearman correlations between SMG1 and all expressed genes were computed across patients. To minimize outlier-driven effects, genes with excessively high variance were filtered out and the correlation centered. Gene Set Enrichment Analysis (GSEA) was then performed on the ranked correlation list, revealing ''RNA splicing'' among the top significantly enriched Gene Ontology (GO) biological processes. The R script is available at https://github.com/Fpastro/Fig.5 git. RNAseq data of the TCGA for correlation studies were obtained from cbioportal (https://www.cbioportal.org/).

QUANTIFICATION AND STATISTICAL ANALYSIS

Obtained data from *in vivo* and *in vitro* experiments was processed with GraphPad Prism 8. All figures show mean ± SEM. Flow cytometry data analysis was performed with FlowJo10. Error bars represent standard error of the mean (SEM) in all plots. One-way ANOVA followed by a *post-hoc* Bonferroni test was performed to analyze statistical differences between independent groups. If experiments had only 2 groups, unpaired two-tailed Student's *t* test was performed instead. For *in vivo* experiments with measures distributed in several time points, significant effect was determined by using two-way ANOVA with Bonferroni test. Statistical significance is considered at $p < 0.05$. When differences are statistically significant, the significance is always represented with asterisks (*) according to the following values: $p < 0.05$ (*), $p < 0.01$ (**), $p < 0.001$ (***) and $p < 0.0001$ (****).